

BOOK OF TUTORIALS AND ABSTRACTS



European Microbeam Analysis Society

EMAS 2009

11th

EUROPEAN WORKSHOP

on

MODERN DEVELOPMENTS

AND

APPLICATIONS

IN

MICROBEAM ANALYSIS

10 to 14 May 2009

at the

Hotel Spa Faltom

Gdynia/Rumia, Gdansk, Poland

Organized in collaboration with
Silesian University of Technology
Polish Society for Microscopy (PTMi)
Polish Academy of Sciences:
Committee of Materials Science, Institute of Physics,
Institute of Materials Science and Metallurgy



THE ROLE OF ATOM-PROBE TOMOGRAPHY IN MATERIALS SCIENCE

Didier Blavette*, E. Cadel, O. Cojocaru-Mirédin and B. Deconihout

University of Rouen, Groupe de Physique des Matériaux, UMR CNRS 6634
P.O. Box 12, FR-76801 St. Etienne du Rouvray Cedex, France

* Institut Universitaire de France

Professor Didier Blavette earned a DEA in Solid State Physics in 1979, a Ph.D. in 1981 and finally, in 1986 he obtained a Doctorat d'Etat (Habilitation). He started his professional career in 1981 as an "Attaché de Recherche" at the C.N.R.S., where in 1984 he became a "Chargé de Recherche". In 1990 he became a Professor at the University of Rouen, where he became an "Exceptional rank Professor" in 2003. He supervised the design and development of the tomographic atom probe (1990-1994). In 2003, he became Head of "Groupe de Physique des Matériaux (UMR CNRS 6634)". Since 2006 he is also Director of "Groupement de Recherche (GDR - CNRS) «TransDiff»". In 2008 he was the Director of the CNRS School «Diffusive phase transformation», held in Porquerolles. He was from 2000 to 2006 a member of the Steering Committee of the International Field Emission Society. He is author or co-author of 200 articles (among them are invited articles or overviews).

In 1988 he received the "Jules Garnier" prize awarded by the French Society for Metallurgy (SF2M). From 1992 to 1997 he was a (Junior) member of "Institut Universitaire de France". In 1993 he was awarded by SF2M, the "Chevenard" medal. In 1995 he received the "Esclangan" prize awarded by the French Society of Physics (SFP). In 2000 he received the "Rocard" prize by SFP. Also in 2000 he was awarded the "Silver medal" of the CNRS. Since 2007 he is a (senior) member of Institut Universitaire de France.

1. ABSTRACT

Three-dimensional atom-probe (3DAP) is the only analytical microscope able to map out the distribution of elements in 3D at the atomic-scale. 3DAP provides quantitative measurements of local chemical composition in a small selected volume. A new generation of instrument, namely, a laser assisted tomographic atom probe (laser-assisted wide-angle atom probe LaWaTAP) has recently been designed in order to open the instrument to bad electric conductors. The use of ultrafast laser pulses rather than of high-voltage pulses to field evaporate surface atoms makes it possible the analysis of semi-conductors or oxides that are key materials in microelectronics. This article is focused on methodology and applications to boron doped silicon. Depth profiles related to boron in various samples (boron deltas, SiGe Maya layers, boron-implanted silicon...) will be discussed and compared to SIMS results. Spatial resolution and sensitivities will be compared.

2. INTRODUCTION

3D atom-probe (3DAP) is an extension in 3D of the atom-probe field ion microscope (APFIM), an instrument designed in the late sixties by E.W. Müller [1]. The two first prototypes were designed successively at the Universities of Oxford and Rouen, the French version being the tomographic atom probe (TAP) [2, 3]. One advantage of 3DAP compared to high-resolution electron microscopy (HREM) is that 3D atom probes have 3D imaging capabilities at the atomic scale. This is the only nanoanalytical microscope able to provide 3D atomic-scale images. It makes it possible to give the spatial distribution of chemical species in the small volume ($50 \times 50 \times 100 \text{ nm}^3$) that is analyzed. One disadvantage compared to HREM is that the spatial resolution ($\sim 0.3 \text{ nm}$ at the specimen surface, 0.1 nm in depth) of 3DAP does not make it possible to image the crystal lattice. Only atomic planes perpendicular to the specimen surface can be resolved. Compared to SIMS, there is no need of calibration of ionisation rates. Provided that experimental conditions are properly settled, composition data are quantitative.

Concentrations in a small selected region (precipitate, interface, defect) can be derived from 3D images. Thanks to its high depth resolution, atomic planes can be imaged and the chemical order can be exhibited in ordered regions. Among the more salient results obtained, let us mention the imaging of Cottrell atmospheres (tiny clouds of impurity atoms around dislocations in crystals). The concept of « atmospheres » was introduced by Cottrell and Bilby [4] in 1949 to explain the role of impurities in the plastic. Thanks to 3DAP, a Cottrell atmosphere in FeAl intermetallics was imaged in 3D and at the atomic scale for the first time [5].

3DAP was up to recently restricted to good conductors (metallic alloys or low-resistance oxides). To overcome this limitation, we designed a new generation of 3DAP in which the material removal is ensured by applying ultrafast laser pulses (350 fs). This new instrument, namely the laser-assisted wide-angle tomographic atom probe (LaWaTAP) opens the field of application of the technique to materials that have a poor electrical conductivity such as semiconductors and oxides, which are key materials in micro-electronics [6]. In this instrument, the evaporation of surface atoms is assisted by femto-second pulses instead of electric pulses [7]. In addition, a wider field of view is achieved in this new instrument so that larger area of analysis are obtained ($50 \times 50 \text{ nm}^2$) improving therefore statistics together with shortening the number of analyses required to get the relevant information. This instrument was developed in collaboration with Cameca, the French company that commercializes the instrument.

With the impressive progresses made in the miniaturisation of integrated circuits, microelectronics occupies a particular place in nanoscience. The size of last generation nanotransistors is a hundred nanometres. SIMS occupies a central position in microelectronics for dopant profiling in semiconductors. However, for nanotransistors SIMS faces its ultimate limits and 3DAP is appealed to play an important role [8]. The Moore law will soon experience new physical limits and new challenges for which the LaWaTAP could bring new and relevant results. More generally, the LaWaTAP appears to be a very powerful approach in nanoscience in particular for the investigation of nanowires and multilayers including tunnel junctions (e.g., MgO/Fe/MgO) containing highly resistive oxide layers [9].

3. LASER-ASSISTED THREE-DIMENSIONAL ATOM PROBE

The principle of the tomographic atom probe is based on the pulsed field evaporation of surface atoms and the identification of field evaporated ions by time of flight mass spectrometry. The in-depth investigation of the sample is provided by the layer-by-layer evaporation of the specimen. The high electric field required (a few tens V/nm) is obtained by applying a high electric voltage (V_0) to the specimen prepared in the form of a sharply pointed needle (tip radius R close to 50 nm, Fig. 1). The chemical identity of atoms is determined by time-of-flight mass spectrometry. High voltage pulses V_p (a few kHz), superimposed to V_0 , lead to the field evaporation of surface atoms as ions. Field evaporated ions are detected on a detector that gives the time of flight (t) of chemical species. The detection efficiency is close to 50 %. However, under proper conditions, the ionisation rate is 100 %. The mass to charge ratio of ions (m/n) is derived from the simple equation $\frac{1}{2} m v^2 = n e (V_0 + V_p)$ with $v = L/t$ (L , the flight path $\sim 10 \text{ cm}$).

A time-resolved position detector makes it possible to position ion impacts and to calculate the position from which atoms originate at the tip surface (Fig. 1). A simple point projection

(close to a stereographic projection) is involved in the reconstruction of the analysed volume. The magnification, close to 10^7 , is simply given by: $G = L/(m + 1)R$, where m defines the position of the centre of projection (CP = mR). Layer after layer, the material that is removed

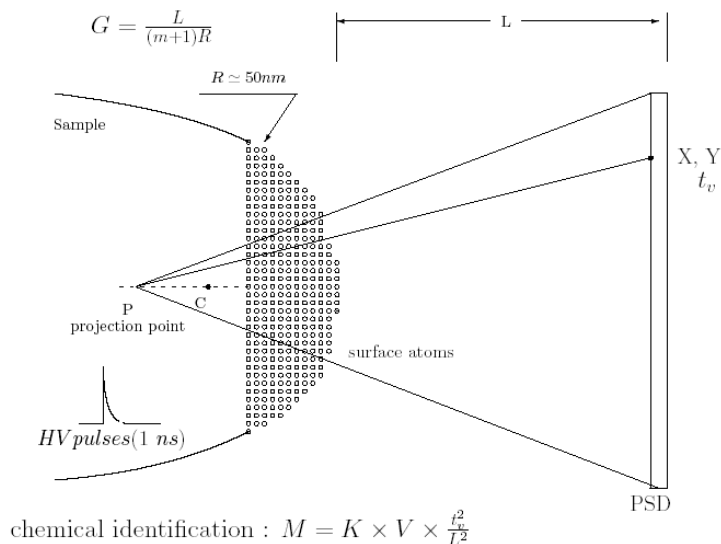


Figure 1. The principle of the tomographic atom probe. In the laser-assisted tomographic atom probe (LaWaTAP), electric pulses are replaced by ultrafast laser pulses (pulse width ranging from 130 to 350 fs).

can be reconstructed. The maximum depth that can be explored with 3DAP is around 1000 nm and the analysed area is a few tens of nm wide (40 - 100 nm). This leads to a reconstructed volume that contains a few tens millions of atoms.

In the first generations of 3D atom-probes, materials with low electrical conductivity could not be analysed properly. High voltage pulses could not be transmitted properly to the tip apex. The broadening of the HV pulse transmitted to the tip apex as well as the lowering of its amplitude lead to very deteriorated mass spectra that were often impossible to index properly. For highly resistive materials, it was even impossible to get any data.

In the laser-assisted wide-angle tomographic atom probe (LaWaTAP, Cameca), HV pulses initially used to field evaporate surface atoms are replaced by femto-second laser pulses. The duration of light pulses is a few hundreds fs and their energy is a few μJ . Kellogg and Tsong [10] were the first, 25 years ago, to implement a pulsed laser one-dimensional atom-probe. However, this idea was never applied to 3D atom-probe until recently. We showed the first results in 2004 at the International Field Emission Symposium [6]. We demonstrated that the use of ultrafast laser pulses allows to field evaporate surface atoms in intrinsic silicon. As

expected, the very short duration of the laser pulse significantly weakens the ion energy distribution leading to a high mass resolution without the need of time focussing or energy compensating devices.

Successful analyses of highly resistive intrinsic silicon posts were performed (Fig. 2). Mass spectra demonstrate that laser pulses greatly improve both the mass resolution ($M/\delta M \sim 1000$) and the signal-to-noise ratio. This leads to a much better sensitivity to low concentrations. The ultimate detection limit of LaWaTAP is a few tens of ppm (i.e., 0.001 at%).

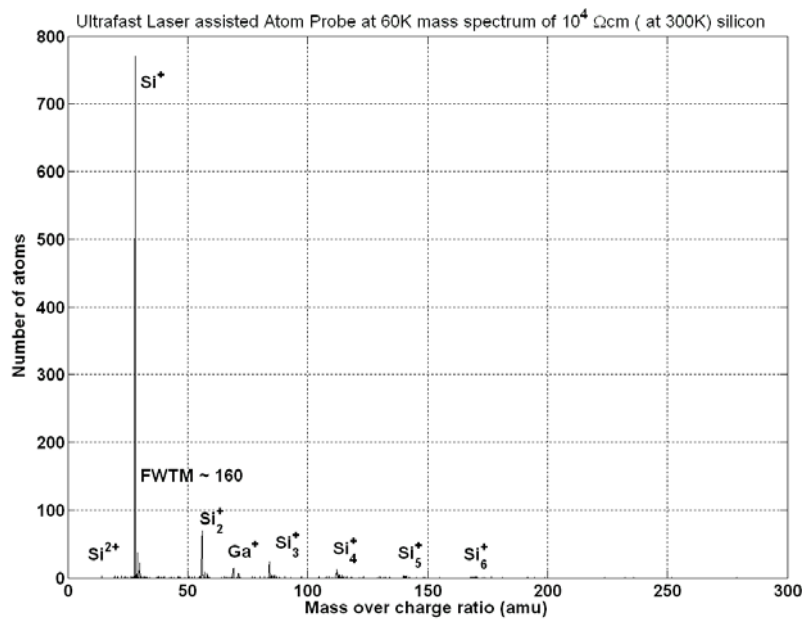


Figure 2. Mass spectrum related to the analysis of intrinsic silicon with a resistivity of $104 \Omega\text{cm}$. Note the presence of Ga ions implanted during ion milling of the specimen using FIB (focussed ion beam) techniques.

The physics of the interaction of ultra-fast laser pulses (a few hundreds fs) with an object having sub-wavelength dimensions is complex and still under debate. It is thought that under specific experimental conditions (small energy/pulse, rather low pulse repetition rate, ...), the evaporation of surface atoms is mainly activated by a field effect and is not thermally activated. We have shown that if the linear polarisation of the laser-wave is set parallel to the tip axis, the rectification of the optical field at the surface generates a rectified ultrafast pulsed field that causes the evaporation of surface atoms [11]. This effect can only take place at the surface of the specimen where the electronic density of states is highly asymmetrical. It means that the pulsed field lies in the very first atomic layers preserving the depth resolution.

4. LASER-ASSISTED THREE-DIMENSIONAL ATOM PROBE VERSUS SIMS

In order to assess the performance of the LaWaTAP, test samples were investigated and results were compared to depth profiles provided by SIMS analysis. Test samples consisted in a stack of 4 thin SiGe layers (thickness close to 10 nm) with increasing Ge concentration (5, 10, 15, 18 at% of Ge). Tips required for atom probe analysis were made using FIB annular milling [12]. The direct comparison of depth profiles provided by LaWaTAP and SIMS shows a very good agreement (Fig. 3). Compositions are observed to be quantitative and the depth scale is shown to be well calibrated. Similar comparisons on ultralow-energy arsenic implants in silicon was made and also revealed good agreement between 3D atom-probe and SIMS [13].

Concentration (atomic %)

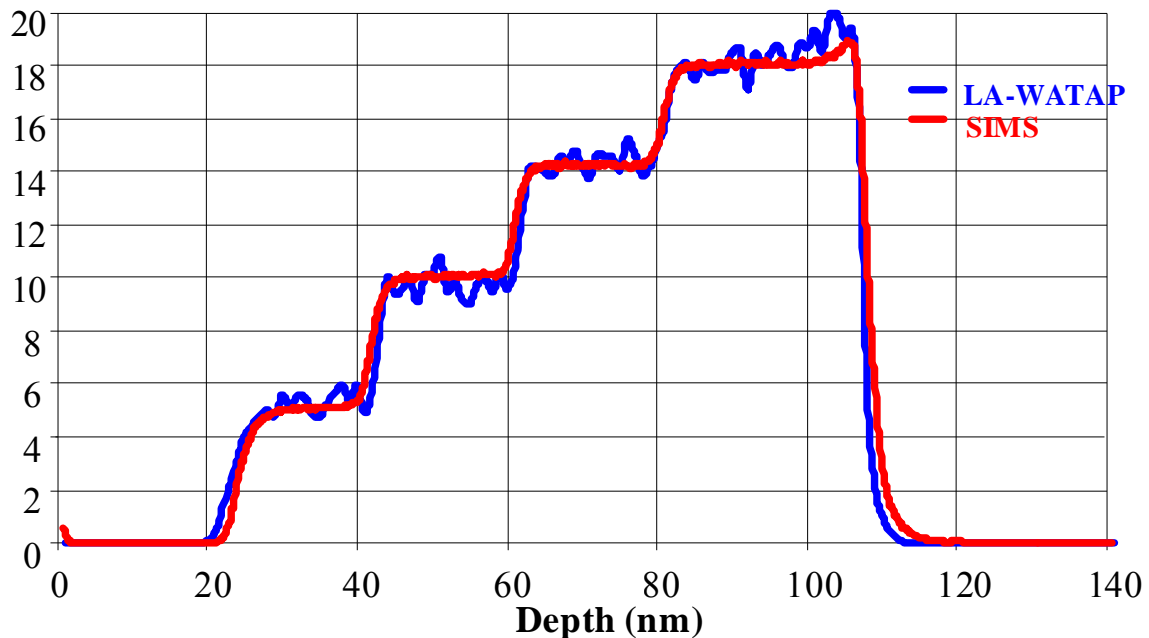


Figure 3. Comparison of concentration profiles related to the analysis of a step-like SiGe multilayer (Maya) using LaWaTAP and SIMS (courtesy Cameca).

However, LaWaTAP has the drawback of its advantage: due to the small analysed area, profiles are shown to be subjected to larger statistical fluctuations. These larger sampling errors ($\sim 2\sigma$ with σ the standard deviation) are caused by the much smaller volume (i.e., smaller number (N) of atoms) on which atom-probe estimates relies. In other words, LaWaTAP has a higher spatial resolution and makes it possible to get concentrations on much smaller volumes. The obvious drawback is that sampling errors are larger.

Statistical fluctuations can easily be assessed. LaWaTAP profiles shown in Fig. 3 were constructed by moving a thin slice (thickness e , d^2 the analyzed area) in a direction perpendicular to multilayer interfaces. The amplitude of sampling errors is given by the standard deviation $\sigma = (C(1 - C)/N)^{1/2}$ with $N = QV/\Omega$ with Q the detection efficiency (~ 0.5), V the volume of slice ($V = e.d^2$) and Ω the average atomic volume ($\sim 0.02 \text{ nm}^3$ in Si). For an analysed area of $d^2 = 20 \times 20 \text{ nm}^2$, a thickness $e = 0.4 \text{ nm}$, one finds $N \sim 4000$ atoms. For a Ge concentration of $C = 10 \%$, $\sigma \sim 0.5 \text{ at\%}$ so that sampling errors ($\sim 2\sigma$) are 1% . This is the order of magnitude of fluctuations observed in depth profile (Fig. 3).

The 3D atomic map of boron atoms in silicon samples containing boron deltas (ultra-thin boron-rich layers) is provided in Fig. 4. Four delta appear in this reconstruction. The related depth profile taken perpendicular to boron layers is compared to SIMS profile in Fig. 5. Again a good agreement is observed. As expected, the boron layers are separated by 18 nm and a peak boron concentration around $10^{21} \text{ boron atoms/cm}^3$ is measured for each delta. Note a slow decrease of the peak concentration in the opposite direction of growth. Let us mention also the larger steepness of LaWaTAP profiles compared to SIMS. Interfaces appear more abrupt, illustrating therefore the higher depth resolution of LaWaTAP. However, the base level of boron between deltas is lower in SIMS profiles. LaWaTAP has a lower sensitivity compared to SIMS. As shown in Fig. 5, the background in this particular experiment was larger than 10^{19} at/cm^3 . A more detailed discussion is available in reference [14].

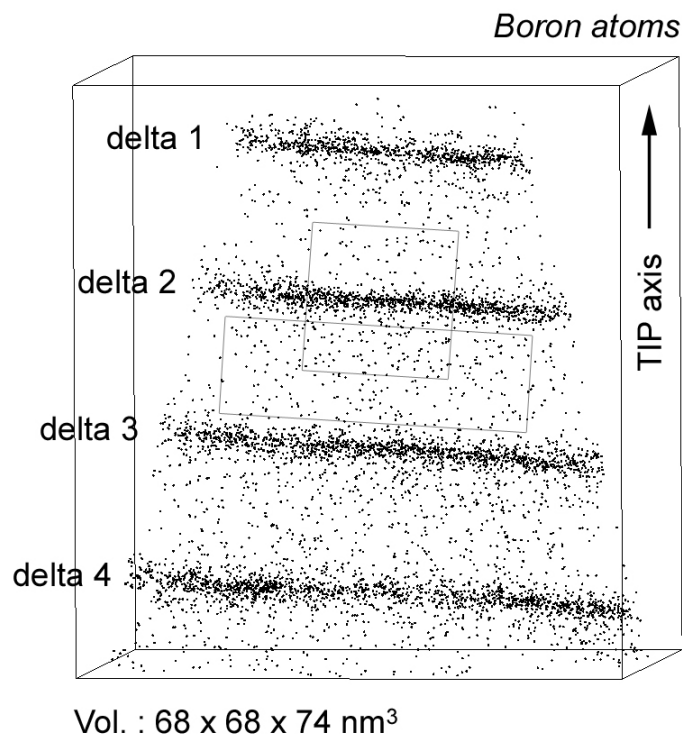


Figure 4. 3D reconstruction of boron distribution in silicon samples. For clarity, only boron atoms are showed. Four boron deltas are exhibited. Layers are separated by 18.3 nm .

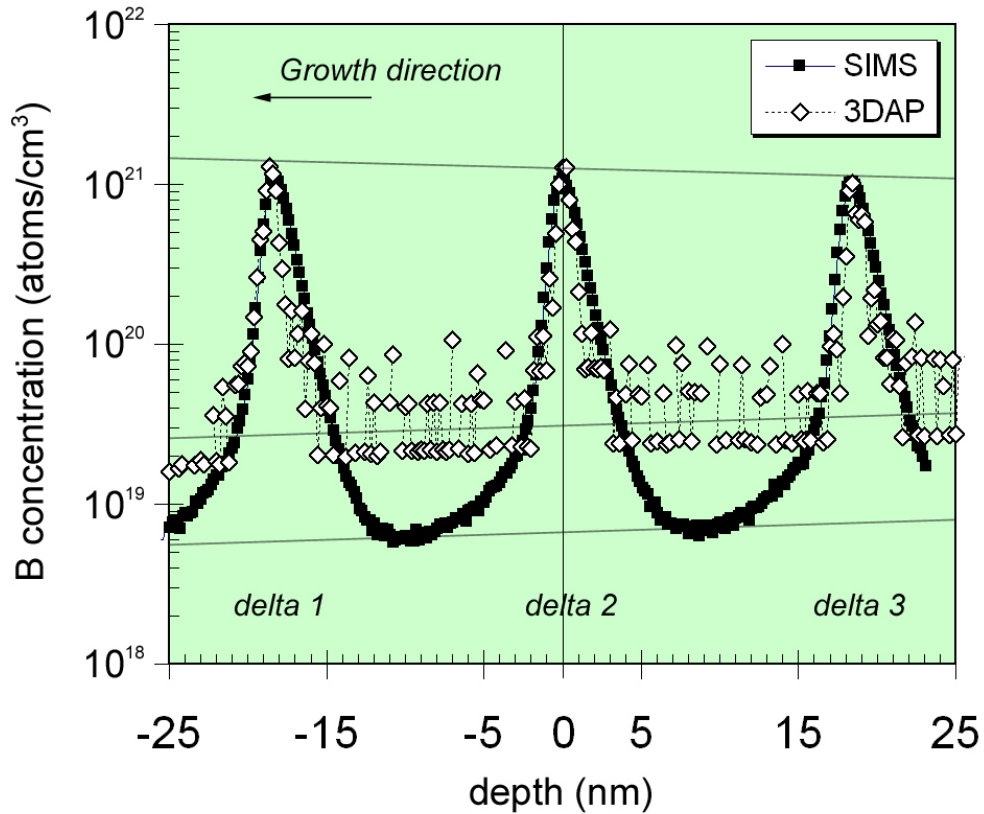


Figure 5. Concentration profile of boron derived from 3D map (Fig. 4). A thin slice 0.2 nm thick was moved in a direction perpendicular to the three first boron deltas. The surface area of the sampling box is 25 nm x 25 nm. SIMS profile is superimposed to that of LaWaTAP.

5. DOPANT DISTRIBUTION IN BORON-IMPLANTED SILICON

Boron implanted silicon with a concentration exceeding the solubility limit has been investigated using LaWaTAP and SIMS. The implantation dose was chosen high (5×10^{15} at/cm², boron ions of 10 keV), close to that of ultra-shallow junctions in last generation nano-transistors. Experiments were conducted on (001) implanted silicon. Mono-isotopic boron implant (¹¹B) was performed on a boron-doped {100} oriented silicon wafer (resistivity 0.01 Ω cm, boron concentration close to 10^{19} at/cm³). High aspect ratio, flat-topped 100 μm tall {100} silicon posts were prepared using Bosch etching techniques [12] on half of the wafer in order to prepare sharp tips for LaWaTAP analyses. Implantation was made on these posts and on the other half of the wafer for SIMS investigations. During ion implantation, the silicon substrate was tilted at 7° off the incident ion beam in order to minimize ion channelling effects.

Thermal annealing for 1 h at 600°C under vacuum at 10^{-6} Torr was then performed to remove implantation damages and activate dopants. A capping layer of silicon (200 nm) was deposited

on top of samples in order to protect the boron implant from being damaged by the focussed ion beam (FIB) milling during sample preparation.

The 3D distribution of boron, oxygen and silicon atoms in the small volume analyzed ($44 \times 44 \times 215.7 \text{ nm}^3$) is shown in Fig. 6. A native oxide (SiO_2 - measured oxygen concentration: 63 at%), 2 nm thick is observed at the surface. Note the drastic decrease of the boron concentration for depth exceeding 100 nm. Numerous platelet-shaped boron clusters containing about fifty atoms (Si and B) were discovered (zoom region in Fig. 6). As expected, the number density is significantly higher in the region where the boron concentration is higher (higher driving force for clustering). The number density of clusters ($\sim 10^{18}$ clusters/ cm^3) is observed to decrease drastically for depth exceeding 100 nm. These clusters have the shape of platelets parallel to the implanted surface, in agreement with BIC's (boron interstitial clusters) observed by Cristiano *et al.* [15]. The average boron content in these clusters as determined from LaWaTAP images was found to be close to 7 at% [16].

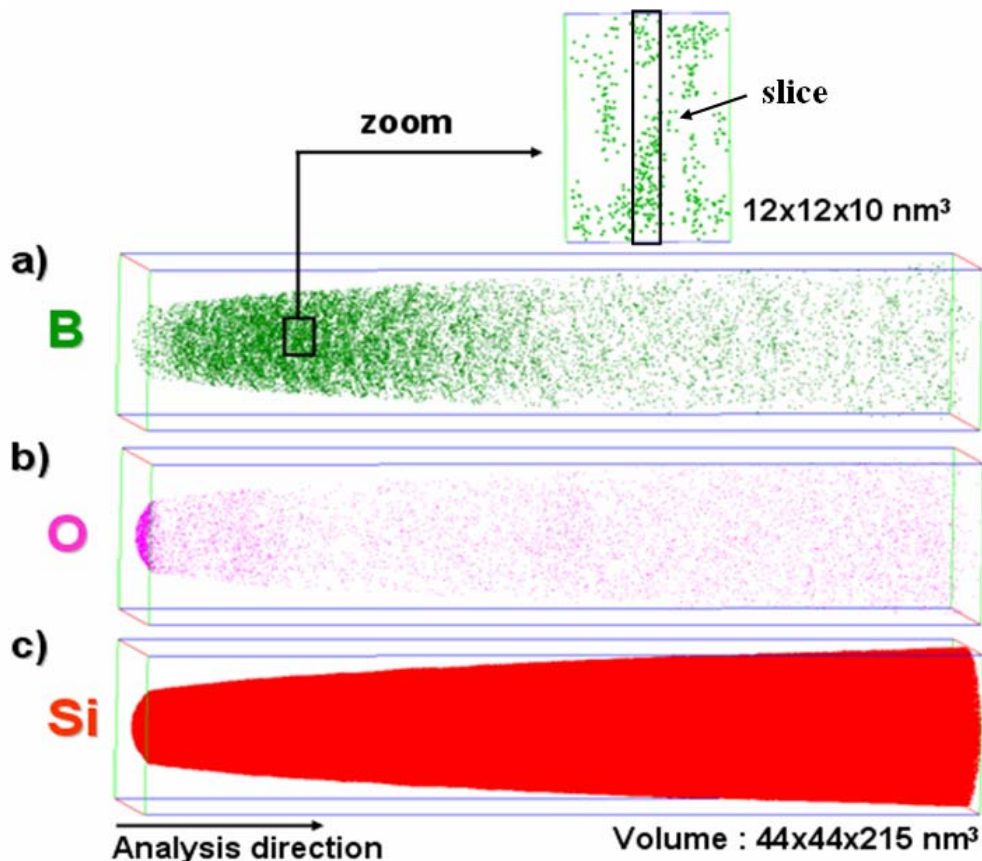


Figure 6. Elemental maps of boron, oxide and silicon in the volume ($44 \times 44 \times 215 \text{ nm}^3$) analysed by LaWaTAP (boron implanted silicon annealed at $600 \text{ }^\circ\text{C}$ for 1 h). A native oxide layer ($\approx 2 \text{ nm}$) is exhibited at the sample surface. The small slice used to construct concentration profile (Fig. 7) is represented in the zoom.

Related concentration profile of boron (in log scale) as derived from Fig. 6 is compared to SIMS profile in Fig. 7. This profile was taken in the Ga-free region of the reconstructed region in order to minimize Ga-irradiation effects. For SIMS analysis (Cameca D-SIMS 7f), the B-profile was measured under vacuum using a primary ion beam of O_2^+ ions with energy of 3 keV and an impact incidence angle of 45° . A fairly good agreement between SIMS and LaWaTAP depth profiles is observed. The maximum concentration (9×10^{20} at/cm³), close for both techniques, is detected at a depth of 35 nm in both APT and SIMS profiles (implantation peak).

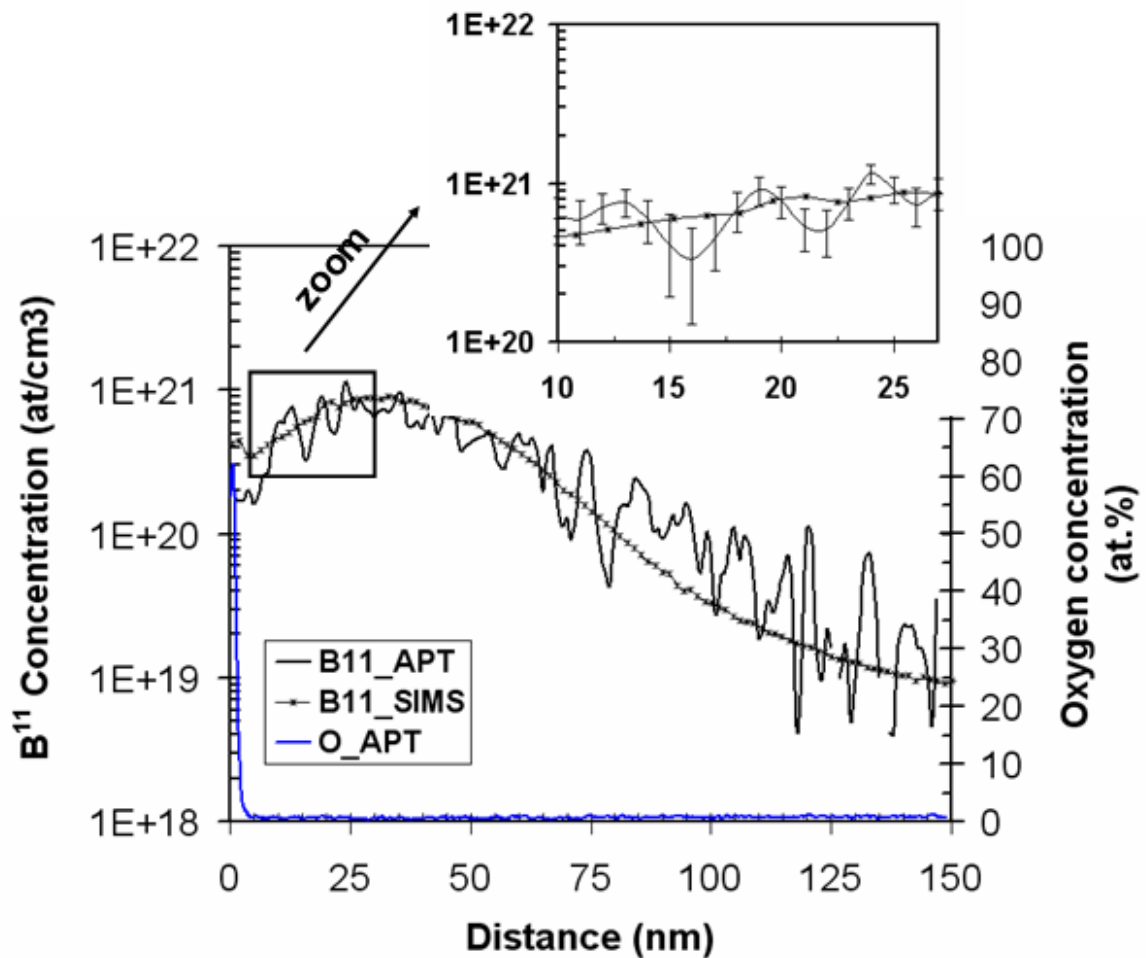


Figure 7. ^{11}B concentration profile as given by SIMS and LaWaTAP (APT: atom probe tomography). LaWaTAP profile reveals the presence of a native oxide at the sample surface. LaWaTAP depth profiles were obtained by moving a small box (2 nm thick and 12 nm wide) through the analyzed volume (Fig. 6) in a direction perpendicular to the sample surface that was exposed to boron implantation.

Significant differences are however apparent. Again, statistical fluctuations appear in the LaWaTAP depth profile. The atom-probe profile gives a boron concentration of 2×10^{20} at/cm³ close to the sample surface whereas the SIMS profile shows a boron concentration twice larger (4.2×10^{20} at/cm³). It is thought that SIMS overestimate boron concentration close to the surface. SIMS is probably less quantitative at the beginning of analysis close to the surface. Moreover, the presence of the native oxide might also have an influence [17].

For larger depth the LaWaTAP profile remains slightly above the SIMS profile. This is thought to be partly due to the back-ground noise contribution in LaWaTAP measurements. The LaWaTAP concentration signal is observed to decrease slowly down to a boron level around $C = 2 \times 10^{19}$ at/cm³ at a depth close to 150 nm. This concentration is equivalent to an atomic fraction $X = C\Omega = 400$ ppm (with $\Omega \sim 2 \times 10^{-2}$ nm³ the atomic volume of Si, $X = 1 \Leftrightarrow 5 \times 10^{22}$ at/cm³). For larger distances (Fig. 6), the boron concentration remains constant and close to the initial boron concentration in the doped Si wafers (10^{19} at/cm³). This concentration is above the detection limits of LaWaTAP.

There are three limitations in the detection of very low concentrations with atom-probe: i) the background noise in the mass spectrum (back ground vacuum, detector noise...), ii) the sampling errors, and iii) the finite number of ions taken into account in concentration calculations (the minimum fraction is obviously $X_m = 1/N$).

The white noise floor (constant in time space) should generally decrease in mass spectra as $1/(M/n)^{1/2}$. The back ground noise is therefore in principle lower for large mass. However, the presence of a large peak (e.g., Si peak here) in the vicinity (this is the case for As but not for B) can limit severely the sensitivity. The density of noise per unit of mass in this experiment, estimated in a region close to boron peaks, was found close to 8×10^{18} at/cm³/a.m.u. (~ 160 ppm/a.m.u). Note that the mass window chosen for boron (both $^{11}\text{B}^{1+}$ and $^{11}\text{B}^{2+}$ peaks) was close to 1 a.m.u. The real boron level as given by the difference between the rough concentration and the noise over 1 a.m.u is therefore 1.2×10^{19} at/cm³, a value close to the amplitude of the SIMS signal (1×10^{19} at/cm³). The presence of this background noise obviously severely affects the accuracy of composition measurements in particular for low levels. It is worth noting that the signal to noise ration (ε) depends on the mass resolution of the instrument. A better mass resolution makes it possible to use a narrower mass window that leads to a lower noise level (the noise related to a Dirac peak in mass spectrum would be null).

In order to interpret more carefully the differences observed in measured concentrations after 75 nm in depth, statistical fluctuations have to be taken into account. Sampling errors in LaWaTAP profiles expressed in atomic fraction (ΔX) are given by the standard deviation σ ($\Delta X \sim 2\sigma$ for 5 % of confidence limit) with $\sigma = (X(1 - X)Q/N)^{1/2}$ with N the number of detected ions (B + Si) contained in the sampling slice used to construct depth profiles. Note that here the detection efficiency ($Q \sim 0.5$) is to be taken into account because it is the statistical

fluctuations on local concentration that we wish to estimate. The average number of ions N contained in the small sampling slice (2 nm thick and 12 nm wide) can be written as: $N = QV/\Omega$ where V is the volume of sampling box (288 nm³). This gives $N = 7200$ ions/slice. The minimum atomic fraction (X_m) that can be detected, independently of statistics limitations, is obviously $X_m = 1/N = 140$ ppm, a value a little bit smaller than the back ground noise (177 ppm).

6. CONCLUSIONS

The much larger area of analysis available (30 times) compared to previous generations of 3D atom-probe and the implementation of ultrafast laser have both provided a new impulse to 3D atom-probe in material science. This innovation has opened more widely the tomographic atom probe to nanosciences, in particular to semiconductors and oxides which are key materials in modern microelectronics. This also provides a high mass resolution. The use of laser pulses instead of electric pulses has incidentally another advantage. It also enables the use of a lower DC field (V_0) that reduces the electrostatic stress. This considerably makes it easier the investigation of brittle metallic alloys (irradiated steels, oxides, titanium, intermetallics, carbides...) that were conventionally subjected to frequent rupture under the cyclic electrostatic stress applied.

SIMS is the traditional instrument used in microelectronics to get implantation profiles. However, this instrument approaches its ultimate limits for the investigation of last MOS-FET transistors the dimensions of which are under 100 nm. Laser-assisted 3D atom-probe should play an increasing role in this field. This instrument has many advantage compared to SIMS (3D imaging, spatial resolution) but it has also several shortcomings or drawbacks (preparation of specimen, mass resolution, statistics and sensitivity). Instruments are in fact less concurrent than complementary. Statistical fluctuations in LaWaTAP are larger because of the smaller volume analysed compared to SIMS (50 μ m in diameter as compared to 50 nm for LaWaTAP). The analysed area of SIMS, around 10⁶ larger, leads to a much better sensitivity. Even if the low ionisation efficiency of SIMS (between 0.1 and 1 %) compared to LaWaTAP (ionisation rate = 1, detection efficiency $Q = 0.5$) reduces the difference of collected ions (N), statistics remain much better in SIMS analysis (a factor close to 30). The ultimate sensitivity of the instrument might approach 10 ppm. However, this advantage is counterbalanced by the higher lateral resolution of LaWaTAP and its 3D imaging capability.

The volumes that are reconstructed with the LaWaTAP (50 x 50 x 100 nm³) or with comparable instruments (the local electrode atom probe (LEAP) developed by IMAGO [13, 18]) have now a size close to that of last generation MOS nanotransistors. Imaging the dopant distribution in 3D at the atomic scale within nano-transistors is now accessible. Making such experiments in real integrated circuits using FIB and lift-out techniques remains however a difficult task and a challenge for future.

7. ACKNOWLEDGEMENTS

Many thanks to Cameca for its financial support and for many fruitful discussions. L. Renaud (Cameca France) is acknowledged for providing results on SiGe multilayers. The authors wish to thank D. Mangelinck (IN2MP, Marseille) for the many fruitful discussions we have had on common researches we made on boron implants in silicon.

8. REFERENCES

- [1] Müller E W, Panitz J and Mc Lane S B (1968) *Rev. Sci. Instrum.* **39**: 83-88.
- [2] Cerezo A, Godfrey I J and Smith G D W (1988) *Rev. Sci. Instr.* **59**: 862-866.
- [3] Blavette D, Bostel A, Sarrau J M, Deconihout B and Menand A (1993) *Nature* **363**: 432-435.
- [4] Cottrell A H and Bilby B A (1949) *Proc. Phys. Soc. Lond.* **A62**: 49.
- [5] Blavette D, Cadel E, Fraczkiwicz A and Menand A (1999) *Science* **17**: 2317-2319.
- [6] Gault B, Vella A, Vurpillot F, Menand A, Blavette D and Deconihout B (2007) *Ultramicroscopy* **107**: 713-720.
- [7] Gault B, Vurpillot F, Vella A, Gilbert M, Menand A and Blavette D (2006) *B. Rev. Sci. Instr.* **77**: 043705.
- [8] Thompson K, Flaitz P L, Ronsheim P, Larson D J and Kelly T F (2007) *Science* **317**: 1370-1374.
- [9] Blavette D, Al Kassab T, Cadel E, Mackel A, Gilbert M, Cojocar O and Deconihout B (2008) *Intern. Journ. Mater. Res.* **99**: 454-460.
- [10] Kellogg G and Tsong T T (1980) *J. Appl. Phys.* **51**: 1184.
- [11] Vella A, Deconihout B, Marrucci L and Santamato E (2007) *Phys. Rev. Lett.* **99**: 046103.
- [12] Larson D J, Foord D T, Petford-Long A K, Liew H, Blamire M G, Cerezo A and Smith G D W (1999) *Ultramicroscopy* **79**: 287.
- [13] Thompson K, Bunton J H, Kelly T F and Larson D J (2006) *J. Vac. Sci. Technol. B* **24**: 412-427.
- [14] Cadel E, Vurpillot F and Deconihout B (2009) *Rev. Sci. Instr.*, submitted.
- [15] Cristiano F, Hebras X, Cherkashin N and Claverie A (2003) *Appl. Phys. Lett.* **83**: 5407.
- [16] Cojocar-Miredin O, Cadel E, Vurpillot F, Mangelinck D and Blavette D (2009) *Scripta Mater.* **60**: 285-288.
- [17] Gurenko A A, Veksler I V, Meixner A, Thomas R, Dorfman A M and Dingwell D B (2005) *Chem. Geol.* **222**: 268-280.
- [18] Kelly T F and Miller M K (2007) *Rev. Sci. Instrum.* **78**: 031101.

